International Journal of ChemTech Research
CODEN (USA): IJCRGG, ISSN: 0974-4290, ISSN(Online):2455-9555
Vol.12 No.03, pp 266-275, 2019

Enhanced the Photovoltaic Performance of Dye Sensitized Solar Cells using Cu and Mn doped CdSe Nanoparticles

I.R. Celine Rose[1]*, A. Jeya Rajendran[1]

[1]Advanced Materials Research laboratory, Department of Chemistry, Loyola College, Chennai-600 034, India

Abstract : Cadmium selenide (CdSe), Cu and Mn-CdSe nanoparticles were synthesized by solvothermal method using polyethylene glycol as a capping agent. The structures, elements, shape and spectral properties of these nanocrystals are investigated. The obtained Cu-CdSe and Mn-CdSe nanocrystal are consistent with the hexagonal wurtzite crystal structure and the crystallite sizes were found to be 13.70 nm, 8.05 nm, and 6.3 nm respectively. The band gap energy was computed from the absorption data as 1.7 eV for CdSe nanoparticles, 2.7 eV and 3.9 eV for Cu and Mn-CdSe nanoparticles respectively. Scanning electron microscope (SEM) illustrated that the dopants adhered to the substrate uniformly and the effective doping was further confirmed by EDX spectral analysis. The solar cell was fabricated using TiO_2 as photoanode, CdSe and Cu, Mn-CdSe as a counter electrode, ruthenium dye as sensitizer and I^-/I_3^- as electrolyte and the maximum conversion efficiency of solar cells were found to be 3.57 % for CdSe, 4.16 % for Cu-CdSe and 5.52 % for Mn-CdSe nanoparticles.
Key words : semiconductors, solvothermal, Cu, Mn-CdSe nanoparticles, solar cell.

Introduction

Semiconducting nanomaterials are promising building block of future generation photovoltaic devices such as dye sensitized solar cell [1], inorganic solar cell [2], and polymer composite solar cell[3]. One-dimensional semiconductor nanoparticles show size dependent structural, morphological, optical and electrical properties, which make them as potential candidate for different applications. Although the thin film solar cells, based on crystalline Si could provide high quantum conversion efficiency, the high cost of semiconductor grade silicon wafers has tuned the attention of researchers towards developing cheaper materials which may be purely inorganic or may contain organic material as an essential part of the device. As a promising alternative to silicon based solar cell, new photovoltaic systems play a vital role in the development of renewable energy.

Doping can alter the physical properties of semiconductor nanostructures in controllable and desirable ways, and it canbe done by wet-chemical and non-wet chemical approaches. For example, electron- and hole-doping performed in the vaporphase can significantly improve semiconductor conductivity and their

DOI= http://dx.doi.org/10.20902/IJCTR.2019.120334

device performance, demonstrated by field-effect transistors fabricated from p-type or n-type Si nanowires [4].In addition to electron- and hole-doping, paramagnetic dopingas become more attractive because paramagnetic-ion-doped semiconductor nanostructures such as dots, rods, wires and films exhibit fascinating properties and potential applications in solar cells [5], bio imaging, spintronics and quantum interference information processing [6]. Doping can change the structural parameters of nanomaterial as well as properties. For example, doping in the semiconductor used for the fabrication of solar cell may protect the material against photo-oxidation and for a magnetic material the doping enhances the quantum mechanical spins of magnetic materials in the nanocrystal.

The power conversion efficiency (PCE) of quantum dot dye sensitized solar cells (QDSSCs) is still lower than that of dye sensitized solar cells (DSSCs). The poor performance of QDSSCs is mainly due to the narrow absorption range of QDs[7], weak electron collection by the TiO_2 from the QDs[8], charge recombination at the QD–electrolyte interface[9], recombination at the interface between the CE (counter electrode) and the electrolyte, andthe difficulty of assembling a sufficiently large number of QDs on a mesoporous TiO_2 matrix to obtain a well-covered monolayer without cluster formation or aggregation[10].DSSCs using ruthenium complex as photo sensitizers such as N_3, N_{719} and black dyes have shown high photo conversion efficiency (PCE) [11-12]. The extent of diffusion of dye to nanocrystalline TiO_2 matrix significantly affects the efficiency and photocurrent in DSSCs. The electron transport from the dye to the nanocrystalline semiconductor interface is a key step in the energy conversion process in which a photoexcited electron in dye molecules are transferred to external circuit through these semiconductor films.

In this paper, CdSe and Cu, Mn-CdSe nanoparticles were prepared via cost effective solvothermal method at 80 ^oC, which were characterized and the quantum conversion efficiency was measured by fabricating solar cell using the CdSe, Cu and Mn-CdSe as photo cathodes which would act as cosenstizer, nanoporous TiO_2 as a photo anode, ruthenium dye as sensitizers and I^-/I_3^- as electrolyte.

Experimental

Preparation of CdSe, Cu-CdSe and Mn-CdSe nanoparticles

Highly pure seleneous acid (99.9%) analytical grade, cadmium acetate dihydrate ($Cd(CH_3COO)_2.2H_2O$), copper chloride hexahydrate ($CuCl_2.6H_2O$), manganous chloride hexahydrate ($MnCl_2.6H_2O$), ethylene glycol ($HOCH_2CH_2OH$) and hydrazine hydrate ($N_2H_4.H_2O$) were used without further purification of analytical grade, purchased from Merck, Germany.

In the synthesis of CdSe, cadmium acetate hexahydrate and selenous acid were taken in 1:1 ratio and dissolved in 50 mL of deionized water by continuous stirring, followed by the addition of capping agent, poly ethylene glycol and the contents were stirred for an hour. The reducing agent, hydrazine hydrate was added with stirring and refluxed at 80 ^oC for 12 h. The precipitate was centrifuged at 3000 rpm for complete separation of CdSe nanoparticles. The synthesis of Cu and Mn-CdSe nanoparticles were accomplished by 3% solution of copper and manganous solution. Finally the precipitate were collected and washed with anhydrous ethanol and hot distilled water, then dried in vaccum at 80 ^oC for 12 h.

Fabrication of solar cell using TiO_2/CdSe flim

TiO_2 paste was prepared by dissolving 0.5 g of TiO_2 in 1mL of water and 1 mL of acetone and coated on fluorine doped tin oxide (FTO) glass (3.5 cm x 2 cm) by doctor blading technique [13] and sintered at 300 ^oC for 3 h. The solar cell was fabricated using CdSe, Cu and Mn-CdSe as a photo cathode and TiO_2as photoanode coated on FTO glass film, ruthenium dye as sensitizer and I^-/I_3^- solution as an electrolyte.

Instrumentation

The synthesized CdSe, Cu and Mn-CdSe samples were characterized by using X-ray diffractometer (MAC Science MO3XHF22) with Cu(Kα) radiation(λ = 1.5405Å) in the 2θ range of 10-80^{o}with a scanning rate of 3 ^{o}/min. Optical UV-vis absorption spectra of CdSe were recorded using (Schimadzu UV-vis 2700 spectrometer). Photoluminescence (PL) spectrum was recorded at room temperature using a Cary-Eclipse (ELO8O83851) spectrometer with an excitation wavelength of 420 nm. Morphology was studied by a scanning

electron microscope SEM.JSM-7000 operating at 10 kV. Dielectric measurement was recorded by using HIOKI3532 50LCR HITESTER impedance analyser. The current- voltage measurement of solar cell was measured by GS610 YOGOKAWA source measure unit.

Results and Discussion

Powder X-ray diffraction analysis

XRD pattern of CdSe and Cu, Mn-CdSe nanoparticles were shown in Fig-1. The peak positions of all the prepared samples can be assigned to (100), (101), (105), (110), (200),(220) and (311) diffraction planes of hexagonal wurtzite structure (JCPDS- ICDD No-08-0459). XRD patterns reveal that the observed broad peaks due to the synthesized particles are in nano nature. The peak broadened with Cu and Mn doped CdSe a nanoparticle increases the full width at half maximum (FWHM) value of the diffraction peak, which reveals the decreasing in the size of the nanoparticles.

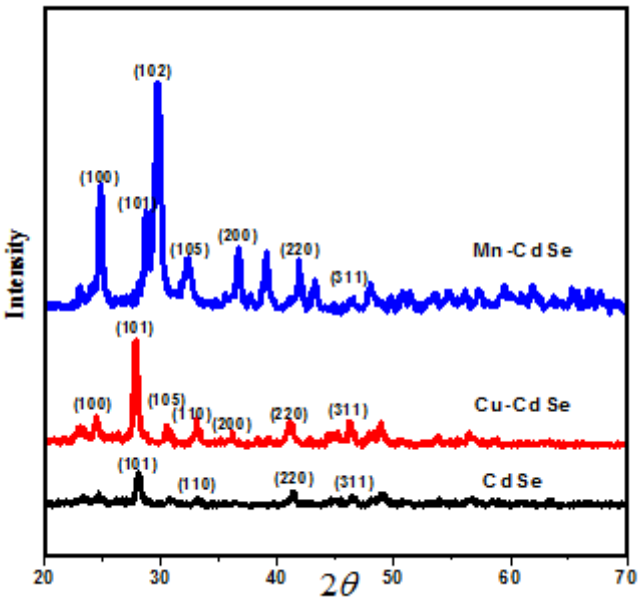

Fig1 XRD spectrum of CdSe and Cu, Mn-CdSe nanoparticles.

Average crystallite size of the prepared samples for the most intense diffraction peak was calculated using Scherer formula [14].

The defects in the nanoparticles can be quantified by computing the dislocation density (δ) which is defined as the length of dislocation lines per unit volume of the crystal [15]. The dislocation density was calculated using the formula given below.

$\delta = 1/D^2$ …….. (1)

This deterioration in crystallinity could be due to the defects and disorders introduce by the dopants in the CdSe structure by segregating into the non-crystalline region at the grain boundary [16] and also due to the strain induced in the lattice by doping. The lattice strain was calculated by using the formula

Lattice strain $\varepsilon = \beta \cos\theta / 4$ …….. (2)

Specific surface area (SSA), a derived scientific value characteristic of the surface was calculated using the formula [16]

Specific surface area $S_a = 6a^3Na/8DM_w$ ……(3)

Where, Na-Avagatro number, M_w- Molecular weight of CdSe, D-average crystallite size

The calculated values of crystallite size (D), dislocation density (δ), strain (ε), lattice parameters (a and c) and surface area were summarized in Table-1. The minimum values of strain and dislocation density were obtained for Mn-CdSe nanoparticles, which enhances the stoichiometry of the nanostructures. The studies on functional dependency of crystallite size, strain, dislocation density with doped nanoparticles represents that the strain and dislocation density decreases, where as the crystallite size increases and the surface area increases

Table 1Structural parameters of CdSe, Cu-CdSe and Mn-CdSe

Sample	D (nm)	δ(x10^{15}m^{-2})	ε	a (Å)	c (Å)	Surface area
CdSe	13.70	9.86	0.002672	3.2481	5.2114	20.43
Cu-CdSe	8.05	7.01	0.002485	3.2561	5.2164	21.48
Mn-CdSe	6.3	5.32	0.002327	3.9134	5.4052	26.19

UV-visible spectral analysis:

Solid state UV-vis absorption spectra was recorded in the region of 200-800 nm(Fig 2),which showed the excitonic peaks at 600 nm, 613 nm and 636 nm for CdSe Cu, and Mn-CdSe nanoparticles. The optical band gap of CdSe nanoparticles were calculated from the absorption peak using the formula

Eg =hc/λ ……(4)

Where h is the Planck's constant, c is the velocity of light and λ is the wavelength at which absorption peaks were obtained. The optical band gap values were found to be 1.7 eV,2.7 eVand3.9 eV for CdSe, Cu-CdSe and Mn-CdSe nanoparticles.

CdSe is a direct band gap semiconductor with band gap of 1.7 eV [17]. The relation between the absorption coefficient (α) and the incident photon energy (hυ) for the case of allowed direct transition using Tauc's relation [17]

$\alpha(h\vartheta) = A(h\vartheta - Eg)^{1/2}$ ……..(5)

$\alpha = 2.3026\ A/t$ …….. (6)

Where A is a absorption coefficient constant, hυ is the photon energy (υ=c/λ, Eg is band gap and n=1/2 for allowed direct transition)

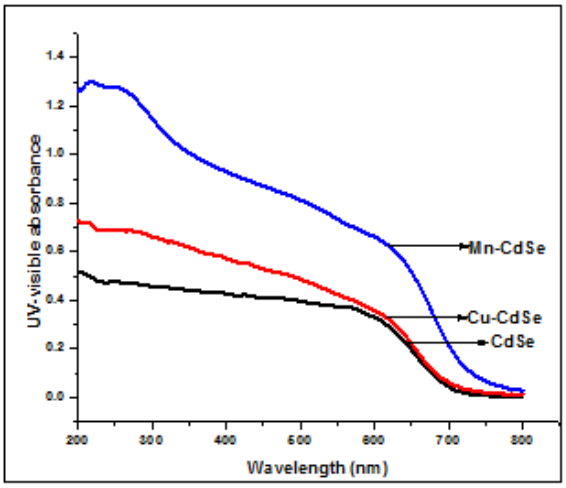

Fig 2 UV-visible absorption spectra of CdSe and Cu, Mn-CdSe nanoparticles

A graph was plotted between ($\alpha h\upsilon^2$) and photon energy ($h\upsilon$)(Fig 3) and extrapolation of the straight line to ($\alpha h\upsilon^2$) = 0, gives the value of band gap. The band gap value was increased from 1.7 eV for CdSe to2.7 eV for Cu-CdSe, and3.9 eV for Mn-CdSe nanoparticles. Increase in the band gap (Eg) accompanied by the quantum size suggests that only photons with higher energy can be absorbed by the quantum dots, leading to a blue shift of the absorption edge of the quantum dots.

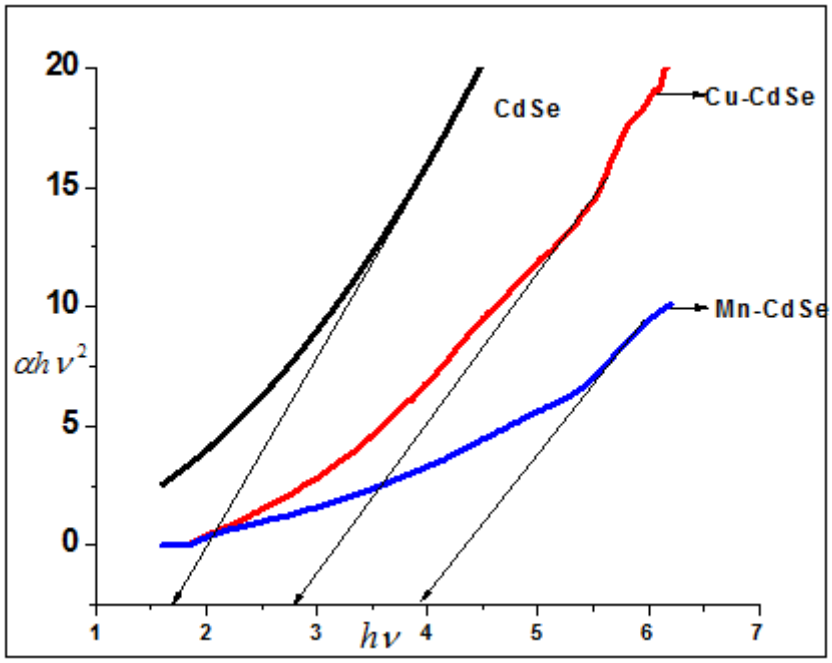

Fig 3 Tauc plot for undoped and Cu, Mn-CdSe nanoparticles

The size of the CdSe nanoparticles were calculated using hyperbolic band model (HBM) using the following equation [18].

$$R = \sqrt{2\pi^2 h^2 E_{gb}}/m^*(E_{gn^2} - E_{gb^2}) \quad \ldots\ldots\ldots\ldots\ldots\ldots (7)$$

Where R is a quantum dot radius (2R is the diameter representing particle size), E_{gb} – Bulk band gap (1.7ev for CdSe),E_{gn}– band gap of nanoparticles (calculated from absorption peak), h–Planck'sconstant, m*-effectivemass (1.18 x 10^{-3}Kg for CdSe).

Table2 The particle size and band gap energy of CdSe Cu, and Mn-CdSe nanoparticles.

Sample(nm)	Band gap energy (ev)	Particle size
CdSe	1.7	14
Cu-doped	2.7	10
Mn-doped	3.9	8.4

The band gap increases as the particle size decreases for transition metal doped CdSe nanoparticles.

Photoluminescence (PL) spectral analysis:

Photoluminescence spectra of the CdSe, Cu and Mn-CdSe nanoparticles (Fig 4) showing two emission bands at 490 nm, weak blue emission band and at ~550 nm, for orange red emission band. The 550 nm emission band was attributed to the d-d transition of Mn^{2+} ion [18]. The emission may be attributed to the relaxation of carriers from excitonic states of host CdSe to T_2 level of dopant Cu. The emission intensity of Mn^{2+} doped CdSe shows maximum luminescence than Cu^{2+} doped CdSe ion, which demonstrates that the

luminescence quantum efficiency of the sample increases to a maximum with the number of unpaired electron in the valence shell of the dopant [18]. The dopant creates electronic states in the mid-gap region of the nanoparticles and thus alters the charge separation and recombination [18]. In addition, the increase in PL enhances the emission of nanoparticles, which leads to the production of more excitations. In a typical PL experiment, a light source was used to excite the nanoparticles that provides photons with energy higher than the band-gap energy. After the photons are absorbed, holes and electrons are formed with finite momenta in the valence and conduction bands, respectively. The photon emission is derived from the recombination of the electrons and holes [19]. The high PL emission value is favorable because more excitons (electrons and holes) results in more recombination of electrons and holes to emit a large number of photons. However, in the DSSCs, the electrons are mainly transferred to electrodes instead of recombination with holes. So high PL intensity would improve the high charge density in the DSSCs [20]. So the dopant Mn^{2+} can accelerate the electron injection from Nanoparticles to TiO_2. This result is consistent with the improvement of absorbance in Mn-CdSe nanoparticles facilitating the transfer of electrons from nanoparticles to TiO_2.

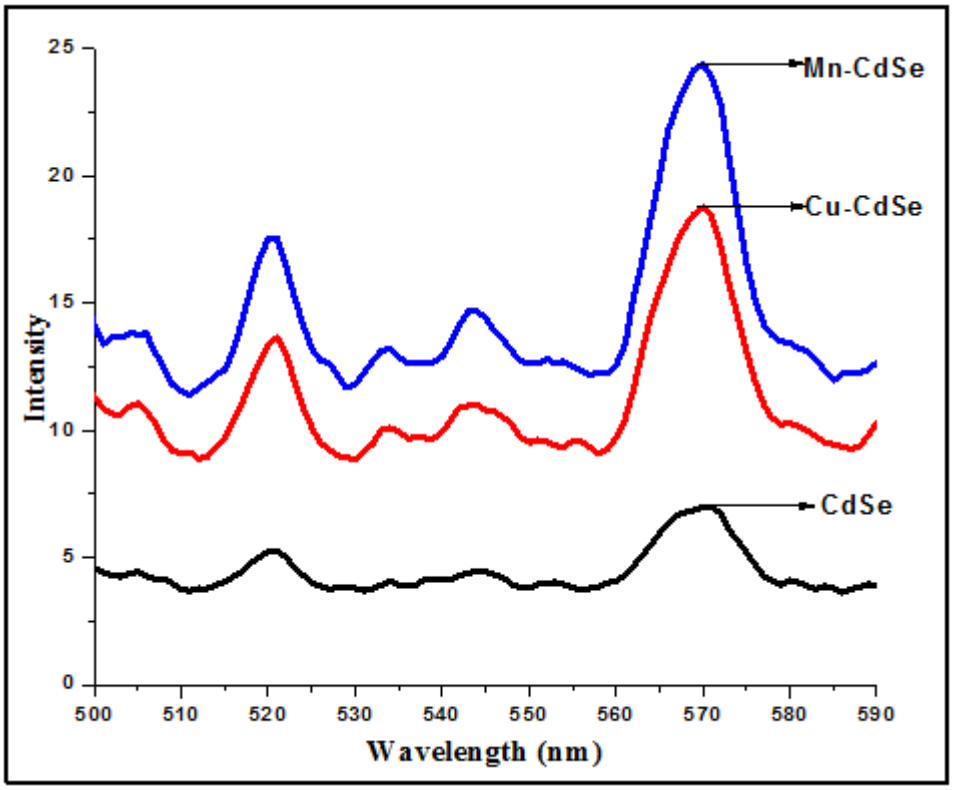

Fig 4 Photoluminescence emission spectra of CdSe Cu and Mn-CdSe nanoparticles

Morphological analysis (SEM)

The scanning electron micrographs of synthesized CdSe, Cu and Mn-CdSe nanoparticles. It shows that pure CdSe nanoparticles(Fig 5(a)) are slightly aggregated phase and well defined structure were observed for 3% doped Cu (Fig 5(b)) and Mn- CdSe 5 (Fig (c)) nanoparticles to favour the formation of flower and spherical morphology. Surface morphology of the material has a significant effect on efficiency of the nanostructure based photovoltaic devices.

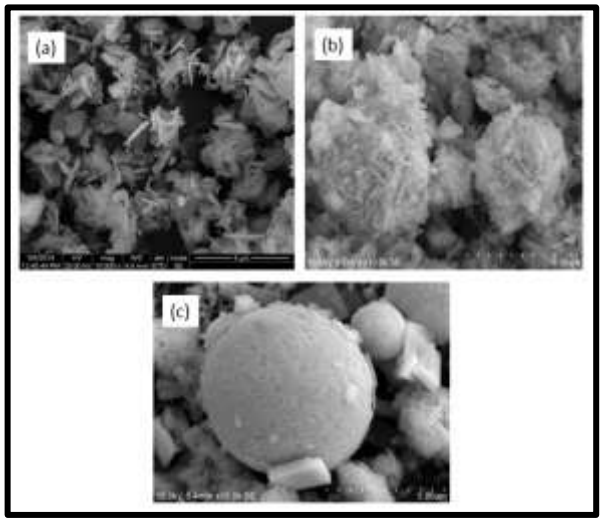

Fig 5 SEM images of (a) CdSe (b) Cu-CdSe (c) Mn-CdSe nanoparticles.

Energy dispersive X-ray analysis

EDX spectra of CdSe, $Cd_{1-x}Cu_xSe$ and $Cd_{1-x}Mn_xSe$ nanoparticles(Fig 6)showing the peaks of cadmium (Cd), selenium (Se) copper (Cu) and manganese (Mn), confirm the presence of Cu and Mn in the host CdSe nanoparticles and the absence of other element as impurity.

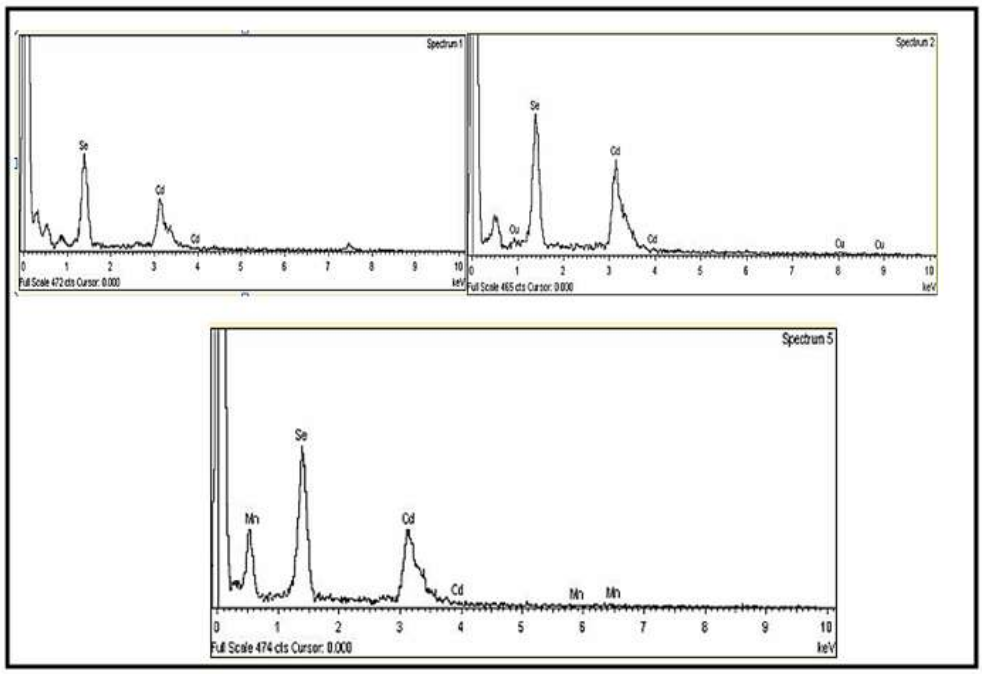

Fig 6 EDX spectral analysis of (a) CdSe (b) Cu -CdSe (c) Mn-CdSe nanoparticles.

Photovoltaic performance:

The photovoltaic performance of solar cell was illustrated by a J-V curve (Fig 7). The photovoltaic parameter, i.e short circuit current(Jsc), open circuit voltage(Voc), fill factor (FF), and power conversion efficiency (η) estimated from these curves are given in table-3. The average short-circuit current (*J*sc) for the cells with Cu and Mn dopant is higher than CdSe, and the Mn-CdSe cells exhibit the highest *J*sc (20mA/cm^2) among all the studied three types of cells (19.2-19.6 mA/cm^2 forother cells). The higher *J*sc in Mn-CdSe cells is the greater light harvesting capacity as indicated by the absorption spectra of the sensitized film electrodes. Meanwhile, the absorbance ratios among different sensitized photocathode are consistent with the

corresponding *J*sc ratios. Besides the enhancement of *J*sc, a distinct improvement of open circuit voltage (*V*oc)has also been observed for cell devices with Mn dopant. Similarly, the Mn-CdSe cells exhibit the highest *V*oc value (1.0 V) among all the cells(0.814-0.9 V for other cells). While, the Mn dopant has no significant influence on fillfactor (FF) of the corresponding cell devices. The enhanced *J*sc and *V*oc, the solar cell with Mn doped CdSe show higher PCEs. Furthermore, the contribution by the Mn-CdSe nanoparticles were greater than that by the CdSe and Cu -CdSe nanoparticles (increase of 3.57% to5.52%).

The efficiency of a solar cell is defined as the output power density divided by the input power density. If the incoming light has a power density P_{in}, the efficiency will be

$$\eta = P_m/P_{in} = Jsc.Voc.FF/P_{in} \quad \ldots\ldots\ldots\ldots\ldots\ldots (8)$$

The fill factor, FF is defined as the ratio of the maximum power output product(P_m) to the product of short circuit photo current and open circuit voltage.

$$FF = \frac{Pm}{Isc\ x\ Voc} = \frac{Imp\ x\ Vmp}{Isc\ x\ Voc} \quad \ldots\ldots\ldots\ldots\ldots\ldots (9)$$

Where I_{mp} and V_{mp} represent the photocurrent and photovoltage corresponding to the maximal power point respectively. The four quantities Jsc, Voc, FF, and η are used to characterize the performance of a solar cell. The photovoltaic parameters are given in table-3.

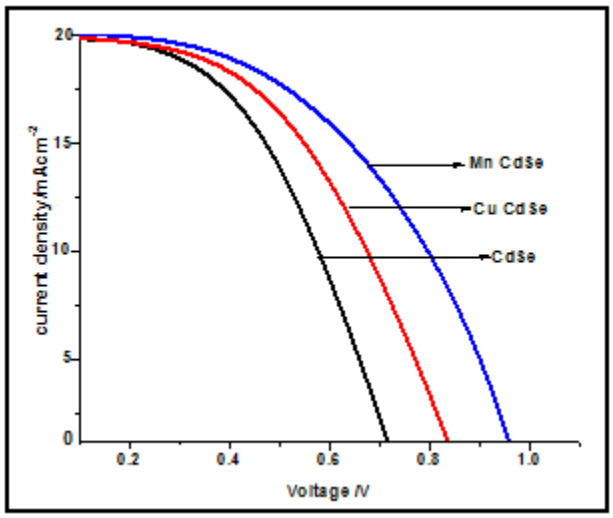

Fig 7 Current –voltage (J-V) curve of CdSe nanoparticles.

Table 3 Photovoltaic parameters of the CdSe based DSSCs.

Parameters	CdSe	Cu-CdSe	Mn-CdSe
Voc [V]	0.8145	0.9	1.0
Jsc [mA]	19.2	19.6	20
FF [%]	0.4798	0.486	0.58
Ŋ [%]	3.57	4.16	5.52

As can be noticed from table-3, there is a relatively improvement of open circuit voltage (Voc) with the effect of synthesized CdSe, Cu and Mn-Cdse nanoparticles compared to both quite stable short circuit current density (Jsc) and fill factor(FF). The increase in the current density (Jsc) and consequently power, could be explained due to the increase in the rate of photoelectrons, whether through a higher generation rate due to optical conversion and the better mobility due to a semiconductive nanostructured materials.

The higher Jsc for the nanoparticles should be ascribed to the broader light harvesting range and higher electron injection rate. While doping with Cu and Mn-CdSe nanoparticles, more light was utilized to generate the photoelectrons resulting in the increment of Jsc which inturn increases quasi Fermi level of TiO_2 by the enhanced injection of photoelectrons from the Co and Ni doped CdSe nanoparticles into the conduction band of TiO_2.

The efficiency of fabricated DSSCs depends on the dopant, as it is obvious from the photovoltaic parameters of the CdSe based DSSCs and the efficiency of the solar cell were improved from 3.57% to 5.52%. Mn-CdSe has the highest Voc and a short circuit current density (Jsc) to others, leading to its better conversion efficiency among these devices. The value of overall power conversion efficiency 3.57% for CdSe, 4.16% for Cu-CdSe and 5.52% for Mn-CdSe nanoparticles respectively.

Conclusion

CdSe, Cu and Mn-cadmium selenide nanoparticles were prepared by solvothermal method at 80^oC for 12 hours. The synthesized samples were characterized by XRD, UV, PL, EDX, and SEM spectral analysis. The powder X-ray diffraction analysis revealed that the synthesized CdSe, Cu-CdSe and Mn-CdSe nanoparticles are in wurtzite structure with average crystallite size of 35.9, 8.05 and 6.3nm. The EDX spectral analysis confirmed the purity of CdSe nanoparticles. The band gap of CdSe nanoparticles were calculated using UV spectral analysis and dielectric studies as 17, 2.7 and 3.9 eV. The well defined morphological SEM image was observed for Cu and Mn-CdSe nanoparticles. The hybrid DSSC using quantum dot CdSe as photocathode, nanocrystalline TiO_2 as photoanode, ruthenium dye as sensitizer, I^-/I_3^- as electrolyte were fabricated and the quantum conversion efficiency of 3.57% for CdSe4.16% for Cu -CdSe and 5.52% for Mn-CdSe nanoparticles.

References

1. Satyajit Saha. Structural and Optical Properties of Chemically Grown CdSe Nanoparticles. J. of Phy. Sci., 2011, 15; 251-254.
2. Murray CB, NorrisDJ, Bawendi MG. Synthesis and characterization of nearly monodisperse CdE (E = S, Se,Te) semiconductor nanocrystallites.J. of Am. Chem. Soc., 1993, 115; 8706–8715.
3. Sreekumaran N,Peining Z,Jagadeesh Babu V,Shengyuanc Y, Seeram Ramakrishna B. Anisotropic TiO2 nanomaterials in dyesensitized solar cells. Phys. Chem. Phys., 2011, 13; 21248–21261.
4. Lee YL, Chang CH. Efficient polysulfide electrolyte for CdS quantum dot-sensitized solar cells. J. of Pow. Sou. 2008, 185; 584–588.
5. Wang H, Bai Y, Zhang H, Zhang Z, Li J, Guo L. CdS quantum dots-sensitized TiO_2 nanorod array on transparent conductive glass photoelectrodes. J. of Phy. Che.C, 2010, 114; 16451–16455.
6. Lee YL, Chi CF, Liau SY. CdS/CdSe co-sensitized TiO_2 photoelectrode for efficient hydrogen generation in a photoelectrochemical cell. Che. of Mater., 2010, 22, 922–927.
7. Chen HS, Su C, Chen JL, Yang TY, Hsu NM, Li WR. Preparation and characterization of pure rutile TiO2 nanoparticles for photocatalytic study and thin films for dye-sensitized solar cells. J. of Nanomater., 2011, 2011;8.
8. Sun M, Chen G, Zhang Y, Wei Q, Ma Z, DuB.Efficient degradation of azo dyes over Sb2S3/TiO2 heterojunction under visible light irradiation. Ind.Eng.che.res., 2012, 51; 2897–2903.
9. Santra PK, Kamat PV. Mn-doped quantum dot sensitized solar cells: a strategy to boost efficiency over 5%. J. of Ame. Che. Soc., 2012, 134; 2508–251.
10. Mocatta D, Cohen G, Schattner J, Millo O, Rabani E, Banin U. Heavily doped semiconductor nanocrystal quantumdots. Science, 2011, 332., 77–81.
11. ChikanV. Challenges and prospects of electronic doping of colloidal quantum dots: case study of CdSe.J. of Phy. Che. Let., 2011, 2; 2783–2789.
12. Reza Amiri1 G, Fatahian S, ahmoudi S. Preparation and Optical Properties Assessment of CdSe Quantum Dots. Mat. Sci. and Appli., 2013, 4, 134-137.
13. TisdaleWA, Williams KJ, TimpBA,NorrisDJ,Aydil ES, Zhu XY, Hot-electron transfer from semiconductor nanocrystals.Science, 2010, 328; 1543–1547.
14. Santanu, ChristopherT, Fadzai F, Pinar D, Viktor C. Progress toward producing n-type CdSe quantum dots: tin and indium doped CdSe quantum dots. J. of Phy. Che. C, 2009, 113; 13008–13015.

15. LeeJW, SonDY, Ahn TK. Quantum-dot-sensitized solar cell with unprecedentedly high photocurrent. Scientific Reports, 2013, 3; article 1050.
16. Wang H, WangBH, HuYX. A method for Co-doped CdSe quantum-dot sensitized TiO_2nano-rod photo-electrodeand its preparation method. China Patent, Application Number 201210234979, July 2012.
17. Wang H, Bai Y, Zhang H, Zhang Z, Li J, Guo L. CdS quantum dots-sensitized TiO_2 nanorod array on transparent conductive glass photoelectrodes. J. of Phy. Che. C, 2010, 114; 16451–16455.
18. Tiwari S. Development of CdS based stable thin film photo electrochemical solar cells. Sol. Ene. Mat. and Sol. Cel., 2006, 90; 1621–1628.
19. De CastroFA, Nuesch F, Walder C, Hany R, Challenges found when patterning semiconducting polymers with electric fields for organic solar cell application. J. of Nanomater, 2012, 2012; 6, Article ID 478296.
20. Farva U, Park C. Colloidal synthesis and air-annealing of CdSe nanorods for the applications in hybrid bulk hetero-junction solar cells. Mat. Lett., 2010, 64, 1415–1417.

*****